

Efficient Evaluation of Singular Integral Equations in Moment Method Analysis of Bodies of Revolution

Úrsula C. Resende*, Fernando J. S. Moreira, and Odilon M. C. Pereira-Filho
*Dept. Electric Engineering, CEFET-MG, Belo Horizonte, MG, CEP 35510-000, Brazil
Dept. Electronics Engineering, UFMG, Belo Horizonte, MG, CEP 31270-901, Brazil
resendeursula@des.cefetmg.br, fernandomoreira@ufmg.br, odilon@cpdee.ufmg.br

Abstract— This work proposes an efficient procedure for evaluating singular integrals arising in the moment method analysis of scattering by bodies of revolution. Perfect electric conductor, dielectric, and composite bodies, varying in size and relative permittivity, are analyzed by the CFIE, Müller, and PMCHWT formulations, respectively. The integrand singularities are extracted and calculated in closed form and numerical integration is applied only for regular functions. It is shown that an efficient singularity removal considerably reduces the number of basis functions required to represent the equivalent current distributions.

Index Terms— Electric and magnetic field integral equations, electromagnetic scattering by bodies of revolution, method of moments.

I. INTRODUCTION

There is a vast literature on methods that use surface integral equations for numerical solution of the electromagnetic scattering by three-dimensional homogeneous bodies [1]-[13]. The efficiency of the method of moments (MoM), applied to solve electric (EFIE) and magnetic (MFIE) field integral equations, in the numerical analysis of the electromagnetic scattering by homogeneous bodies of revolution (BOR) was satisfactorily demonstrated [4]-[9]. Several linear combinations between EFIE and MFIE have been investigated and the most used are the combined field integral equation (CFIE), the PMCHWT (named after Poggio, Miller, Chang, Harrington, Wu, and Tsai), and the Müller formulation. The CFIE is generally applied in the analysis of closed PEC (perfect electric conductor) bodies, while PMCHWT and Müller are generally used in the analysis of dielectric and composite bodies.

In the MoM technique, the choice of basis functions, for the representation of the equivalent surface currents, and testing (weighting) functions is very important in the accuracy and convergence of the numerical analysis. However, sophisticated basis or testing functions may lead to complicated integrands and, consequently, singularity removals. To attain accurate numerical solutions considerable precautions must be taken with the singularity removal. In the present work a robust numerical technique is proposed to remove the singularities arising in the integral equations of the

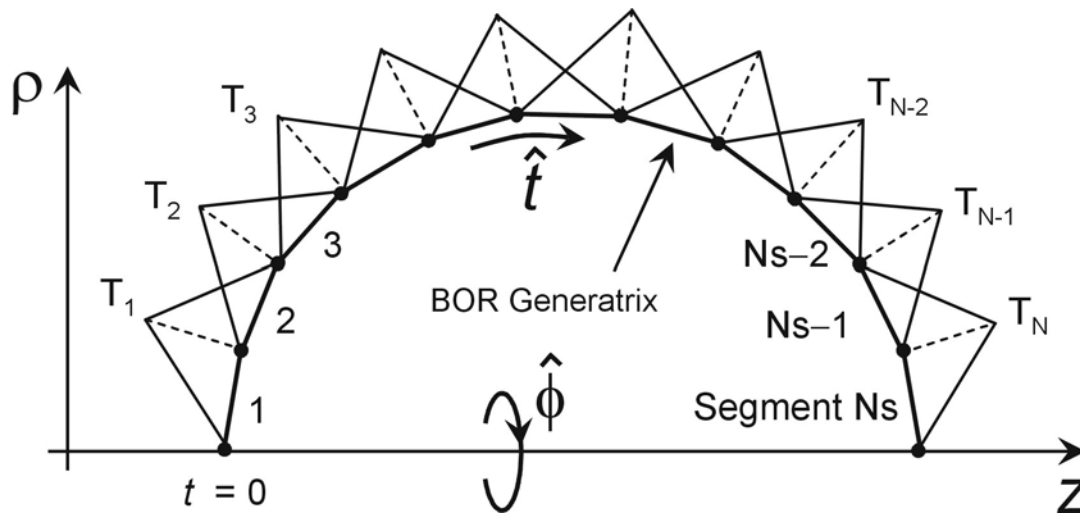


Fig. 1. Triangular basis functions (TBF).

electromagnetic scattering by BOR, suited for triangular basis (and testing) functions (TBF) [8],[9]. The TBF generally guarantees a good representation of current physical behavior and provides relatively simple integrands in the MoM analysis. In the present work, a TBF is defined over two consecutive segments of the BOR generatrix to represent the current surface distributions in both \hat{t} and $\hat{\phi}$ directions, as illustrated in Fig. 1. Galerkin method is used in the MoM analysis and, consequently, the testing functions are defined likewise.

An efficient way to numerically remove the singularities is to apply the extraction technique. The technique was used in [4] and [5], where triangular and pulse functions represent the equivalent surface currents in \hat{t} and $\hat{\phi}$ directions, respectively, and in [10], where RWG functions (named after Rao, Wilton, and Glisson) were employed. In the present work the extraction technique is extended in order to handle the singularities arising whenever TBF's are used to represent both \hat{t} and $\hat{\phi}$ oriented currents with Galerkin technique (i.e., triangular functions are also used to represent the testing functions in both \hat{t} and $\hat{\phi}$ directions). Gaussian quadrature is applied to evaluate integrals with regular kernels. This is discussed in Sects. II and III.

In order to illustrate the accuracy and usefulness of the method, spherical PEC, dielectric, and composite bodies are analyzed in Sect. IV, with spherical radii up to $50\lambda_0$ (where λ_0 is the wavelength in vacuum) and relative permittivities varying up to 50.

II. EFIE AND MFIE FORMULATIONS FOR BOR'S

For a homogeneous BOR (region $i = 1$) with permittivity ϵ_1 and permeability μ_1 , immersed in an infinite and homogeneous medium (region $i = 0$) with permittivity ϵ_0 and permeability μ_0 , the

equivalence principle can be applied to establish a set of four integral equations (EFIE's and MFIE's for the regions inside and outside the body) to solve for the electric (\mathbf{E}) and magnetic (\mathbf{H}) fields in terms of equivalent electric (\mathbf{J}) and magnetic (\mathbf{M}) surface currents. Assuming that the sources of the incident field ($\mathbf{E}^{\text{inc}}, \mathbf{H}^{\text{inc}}$) are outside the body, the integral equations for the tangential field components can be represented, following the notation in [8] and [9], as:

$$[\eta_0 \mathbf{L}_0(\mathbf{J}) + \mathbf{K}_0(\mathbf{M})]_{\text{tan}} = \mathbf{E}_{\text{tan}}^{\text{inc}}, \quad (1)$$

$$[\mathbf{L}_0(\mathbf{M}) - \eta_0 \mathbf{K}_0(\mathbf{J})]_{\text{tan}} = \mathbf{H}_{\text{tan}}^{\text{inc}}, \quad (2)$$

$$[\eta_1 \mathbf{L}_1(\mathbf{J}) + \mathbf{K}_1(\mathbf{M})]_{\text{tan}} = 0, \quad (3)$$

$$[\mathbf{L}_1(\mathbf{M}) - \eta_1 \mathbf{K}_1(\mathbf{J})]_{\text{tan}} = 0, \quad (4)$$

where the index i represents the interior ($i = 1$) and exterior ($i = 0$) regions and η_i is the intrinsic impedance of region i . In (1)-(4), the surface integral operators \mathbf{L}_i and \mathbf{K}_i are defined as [8],[9]:

$$\mathbf{L}_i(\mathbf{X}) = \frac{j}{4\pi k_i} \iint_{S'} [k_i^2 \mathbf{X}(\mathbf{r}') G_i(\mathbf{r}, \mathbf{r}') - \nabla' \mathbf{X}(\mathbf{r}') \nabla' G_i(\mathbf{r}, \mathbf{r}')] ds', \quad (5)$$

$$\mathbf{K}_i(\mathbf{X}) = \nu_i \hat{n} \times \frac{\mathbf{X}(\mathbf{r})}{2} + \frac{1}{4\pi} \iint_{S'} [\mathbf{X}(\mathbf{r}') \times \nabla' G_i(\mathbf{r}, \mathbf{r}')] ds', \quad (6)$$

where the integration limit S' denotes the BOR surface, \hat{n} is the unit outward normal to the BOR surface, k_i is the wave number of region i , \mathbf{X} represents either \mathbf{J} or \mathbf{M} , $\nu_i = 1$ (or -1) if the observation point resides on the outer (or inner) surface of the BOR, and

$$G_i(\mathbf{r}, \mathbf{r}') = \frac{e^{-jk_i |\mathbf{r} - \mathbf{r}'|}}{|\mathbf{r} - \mathbf{r}'|} \quad (7)$$

is the free-space Green's function of region i .

The equations (1)-(4) can be linearly combined in several ways to provide a set of two integral equations to solve for the unknowns \mathbf{J} and \mathbf{M} . For closed PEC bodies (where $\mathbf{M} = 0$) the CFIE formulation is generally adopted [6]. The CFIE is given by the following combination:

$$\alpha' \text{EFIE}_0 + \beta' \text{MFIE}_0, \quad (8)$$

where EFIE_0 and MFIE_0 represent (1) and (2), respectively, and α' and β' are the linear combination weights. For dielectric bodies (where both \mathbf{J} and \mathbf{M} must be determined) the usual linear combinations are of the form [7]-[11]

$$\text{EFIE}_0 + \alpha \text{EFIE}_1, \quad (9)$$

$$\text{MFIE}_0 + \beta \text{MFIE}_1, \tag{10}$$

where EFIE₁ and MFIE₁ represent (3) and (4), respectively. In (9) and (10), $\alpha = -\epsilon_1/\epsilon_0$ and $\beta = -\mu_1/\mu_0$ for the Müller formulation, while $\alpha = \beta = 1$ for the PMCWHT formulation [7]-[11].

Adopting the TBF's to represent the surface equivalent currents, as illustrated in Fig. 1, **J** and **M** are written as [8],[9]:

$$\mathbf{X}(\mathbf{r}') = \sum_{n=-\infty}^{\infty} \left[\sum_{j=1}^{N_t} I_{jn}^{X_t} \frac{T_j^t(t')}{\rho'} \hat{t}' + \sum_{j=1}^{N_\phi} I_{jn}^{X_\phi} \frac{T_j^\phi(t')}{\rho'} \hat{\phi}' \right] e^{-jn\phi'}, \tag{11}$$

where **X** represents either **J** or **M**, \hat{t}' and $\hat{\phi}'$ are the orthogonal unit directions tangential to the BOR surface at the source point \mathbf{r}' , $T_j^t(t')$ and $T_j^\phi(t')$ are the TBF's representing the \hat{t}' and $\hat{\phi}'$ oriented currents, N_t and N_ϕ are the number of TBF's representing the \hat{t}' and $\hat{\phi}'$ oriented currents, respectively, and $I_{jn}^{X_\phi}$ and $I_{jn}^{X_t}$ are the unknown coefficients of $T_j^t(t')$ and $T_j^\phi(t')$ of **X** (i.e., **J** or **M**). In (11), the terms $e^{-jn\phi'}$ correspond to the Fourier expansion in ϕ' , while the division of the TBF's by ρ' prevents singularity problems at the symmetry axis ($\rho' = 0$) [8].

Substituting (11) into (8), for closed PEC bodies, or into (9) and (10), for dielectric and composite bodies, and further applying Galerkin method, the unknown currents can be numerically determined via the well-known MoM technique. In order to illustrate the singularity removal by means of the extraction technique, only the EFIE₀ of (1) will be considered next. However, the singularities arising in (2)-(4) are of the same type and there will be no loss of generality. Therefore, after the MoM linearization, (1) can be represented by the following matrix equation:

$$\begin{bmatrix} V^{E_t} \\ V^{E_\phi} \end{bmatrix} = \eta_0 \begin{bmatrix} Z^{E_{tt}} & Z^{E_{t\phi}} \\ Z^{E_{\phi t}} & Z^{E_{\phi\phi}} \end{bmatrix} \begin{bmatrix} I^{J_t} \\ I^{J_\phi} \end{bmatrix} + \begin{bmatrix} Y^{E_{tt}} & Y^{E_{t\phi}} \\ Y^{E_{\phi t}} & Y^{E_{\phi\phi}} \end{bmatrix} \begin{bmatrix} I^{M_t} \\ I^{M_\phi} \end{bmatrix}, \tag{12}$$

where η_0 is the intrinsic impedance of medium $i = 0$, V^{E_t} and V^{E_ϕ} are the excitation matrix elements and $Z^{E_{t\phi}}$, $Z^{E_{\phi t}}$, $Z^{E_{\phi\phi}}$, $Y^{E_{tt}}$, $Y^{E_{t\phi}}$, $Y^{E_{\phi t}}$, and $Y^{E_{\phi\phi}}$ are sub-matrices of the Z and Y matrices, respectively, which elements are given by [8]:

$$Z_{ij}^{E_{tt}} = j \int_{t'} \int_t \left\{ k_0^2 T_i^t(t) T_j^t(t') [\sin u' \sin u G_5(t, t') + \cos u \cos u' G_7(t, t')] - \frac{\partial T_i^t}{\partial t} \frac{\partial T_j^t}{\partial t} G_7(t, t') \right\} dt' dt, \tag{13}$$

$$Z_{ij}^{E_{t\phi}} = \int_{t'} \int_t \left[k_0^2 T_i^t(t) T_j^\phi(t') \sin u G_6(t, t') + m \frac{\partial T_i^t}{\partial t} \frac{T_j^\phi(t')}{\rho'} G_7(t, t') \right] dt' dt, \tag{14}$$

$$Z_{ij}^{E\phi t} = - \int_t \int_{t'} \left[k_0^2 T_i^\phi(t) T_j^t(t') \sin u' G_6(t, t') + m \frac{T_i^\phi(t)}{\rho} \frac{\partial T_j^t}{\partial t} G_7(t, t') \right] dt' dt, \quad (15)$$

$$Z_{ij}^{E\phi\phi} = j \int_t \int_{t'} \left[k_0^2 T_i^\phi(t) T_j^\phi(t') G_5(t, t') - m^2 \frac{T_i^\phi(t)}{\rho} \frac{T_j^\phi(t')}{\rho'} G_7(t, t') \right] dt' dt, \quad (16)$$

$$Y_{ij}^{E\eta} = j \int_t \int_{t'} k_0^3 T_i^t(t) T_j^t(t') [\rho \cos u \sin u' - \rho' \cos u' \sin u - (z - z') \sin u \sin u'] G_3(t, t') dt' dt, \quad (17)$$

$$Y_{ij}^{E\iota\phi} = \pi \int_t \frac{T_i^t(t) T_i^\phi(t)}{\rho} dt + \int_t \int_{t'} k_0^3 T_i^t(t) T_j^\phi(t') \times \{ \rho' \cos u G_1(t, t') - [(\rho - \rho') \cos u - \sin u (z - z')] G_2(t, t') \} dt' dt, \quad (18)$$

$$Y_{ij}^{E\phi t} = -\pi \int_t \frac{T_i^\phi(t) T_i^t(t)}{\rho} dt + \int_t \int_{t'} k_0^3 T_i^\phi(t) T_j^t(t') \times \{ \rho \cos u' G_1(t, t') + [(\rho - \rho') \cos u' - \sin u' (z - z')] G_2(t, t') \} dt' dt, \quad (19)$$

$$Y_{ij}^{E\phi\phi} = j \int_t \int_{t'} k_l^3 T_i^\phi(t) T_j^\phi(t') (z - z') G_3(t, t') dt' dt, \quad (20)$$

where the indices i and j represent the TBF ordering associated with the testing and basis functions, respectively, u (u') is the angle between \hat{t} and \hat{z} (\hat{t}' and \hat{z}'), and

$$G_1(t, t') = 2 \int_0^\pi \sin^2\left(\frac{\varphi}{2}\right) \cos m\varphi G_H d\varphi, \quad (21)$$

$$G_2(t, t') = \int_0^\pi \cos \varphi \cos m\varphi G_H d\varphi, \quad (22)$$

$$G_3(t, t') = \int_0^\pi \sin \varphi \sin m\varphi G_H d\varphi, \quad (23)$$

$$G_4(t, t') = 2 \int_0^\pi \sin^2\left(\frac{\varphi}{2}\right) \cos m\varphi G_E d\varphi, \quad (24)$$

$$G_5(t, t') = \int_0^\pi \cos \varphi \cos m\varphi G_E d\varphi, \quad (25)$$

$$G_6(t, t') = \int_0^\pi \sin \varphi \sin m\varphi G_E d\varphi, \quad (26)$$

$$G_7(t, t') = G_4(t, t') + G_5(t, t'), \quad (27)$$

with m corresponding to the azimuthal current and field variations, $\varphi = \phi - \phi'$, G_0 is defined in (7),

$$G_E(t, t', \varphi) = \frac{e^{-jk_0 R}}{k_0 R}, \quad (28)$$

$$G_H(t, t', \varphi) = \left[\frac{1 + jk_0 R}{(k_0 R)^2} \right] G_E(t, t', \varphi), \quad (29)$$

$$R = |\mathbf{r} - \mathbf{r}'| = \sqrt{(\rho - \rho')^2 + (z - z')^2 + 4\rho\rho' \sin^2\left(\frac{\phi - \phi'}{2}\right)}. \quad (30)$$

By an appropriate change of variables, the coordinates t and t' can be parameterized as functions of variables α and α' , in the following way [8]:

$$t' = t_q + \alpha' \frac{\Delta_q}{2}, \quad (31)$$

$$t = t_p + \alpha \frac{\Delta_p}{2}, \quad (32)$$

where the indices q and p identify the parameters associated with source and observation segments, respectively, Δ_q and Δ_p are the lengths of the source and observation segments, respectively, and t_q and t_p are central-point coordinate of the source and observation segments, respectively. Consequently, $\alpha, \alpha' = 0$ represent the centers of the segments while $\alpha, \alpha' = \pm 1$ represent their extremities. From (31) and (32), the cylindrical coordinates of the source (primed) and observation (unprimed) points can be represented as [8]:

$$\rho' = \rho_q + \alpha' \frac{\Delta_q}{2} \sin u_q, \quad (33)$$

$$z' = z_q + \alpha' \frac{\Delta_q}{2} \cos u_q, \quad (34)$$

$$\rho = \rho_p + \alpha \frac{\Delta_p}{2} \sin u_p, \quad (35)$$

$$z = z_p + \alpha \frac{\Delta_p}{2} \cos u_p, \quad (36)$$

where z_q and ρ_q (z_p and ρ_p) are the coordinates of the source (observation) segment central point and u_q (u_p) is the angle of the source (observation) segment with the z axis. From (31) and (32), the triangular functions and their derivatives can be represented as [8]:

$$T_j(t') = \frac{1 - (-1)^{iq} \alpha'}{2}, \quad (37)$$

$$T_i(t) = \frac{1 - (-1)^{ip} \alpha}{2}, \quad (38)$$

$$\frac{\partial T_j}{\partial t'} = \frac{-(-1)^{iq}}{\Delta_q}, \quad (39)$$

$$\frac{\partial T_i}{\partial t} = \frac{-(-1)^{ip}}{\Delta_p}, \quad (40)$$

where the index iq (ip) is equal to 1 or 2 for the half-triangle of T_j (T_i) to the right or left of the source (observation) segment, respectively.

III. SINGULARITY EXTRACTION

The integrals in (13)-(20) have removable singularities that arise whenever the observation point \mathbf{r} (unprimed coordinates) is very close to the source point \mathbf{r}' (primed coordinates), i.e., when $R \rightarrow 0$. In this section, an extraction method for the singularity numerical removal will be discussed. The technique is based on those used in [4] and [5], but extended in order to handle the singularity problems arising in (13)-(20), i.e., when triangular functions are used to represent all basis and testing functions. It is anticipated that Gaussian quadratures are employed for regular kernels.

Following the steps in [4], the extraction method is employed in 3 different situations (hereinafter named methods 1, 2, and 3).

A. Method 1

Method 1 is applied when the following conditions are met:

$$R_c \leq C_t \frac{\Delta_q}{2}, \quad (41)$$

$$R_c \geq C_\phi \rho_q, \quad (42)$$

where

$$R_c = \sqrt{(\rho_p - \rho_q)^2 - (z_p - z_q)^2} \quad (43)$$

is the distance between the centers of the source (q) and observation (p) segments of the BOR generatrix (i.e., measured over a constant- ϕ semi-plane), $C_t = 2$, and $C_\phi = 0.1$ [4]. In this case, source and field segments are close to each other and both are close to the symmetry axis. Thus, numerical evaluation of the α' integrals may provide inaccurate results due to the large variation of R in the limit $\phi \rightarrow 0$. In (13)-(20) the α' integrals have the following forms:

$$G_a^{1Z} = \int_{-1}^1 G_E d\alpha' = G_{a1}^{1Z} + G_{a2}^{1Z} = \int_{-1}^1 (G_E - G_E^\Delta) d\alpha' + \int_{-1}^1 G_E^\Delta d\alpha', \quad (44)$$

$$G_b^{1Z} = \int_{-1}^1 G_E \alpha' d\alpha' = G_{b1}^{1Z} + G_{b2}^{1Z} = \int_{-1}^1 (G_E - G_E^\Delta) \alpha' d\alpha' + \int_{-1}^1 G_E^\Delta \alpha' d\alpha', \quad (45)$$

$$G_a^{2Z} = \int_{-1}^1 \frac{G_E}{\rho'} d\alpha' = G_{a1}^{2Z} + G_{a2}^{2Z} = \int_{-1}^1 \frac{1}{\rho'} (G_E - G_E^\Delta) d\alpha' + \int_{-1}^1 \frac{G_E^\Delta}{\rho'} d\alpha', \quad (46)$$

$$G_b^{2Z} = \int_{-1}^1 G_E \frac{\alpha'}{\rho'} d\alpha' = G_{b1}^{2Z} + G_{b2}^{2Z} = \int_{-1}^1 (G_E - G_E^\Delta) \frac{\alpha'}{\rho'} d\alpha' + \int_{-1}^1 G_E^\Delta \frac{\alpha'}{\rho'} d\alpha', \quad (47)$$

$$G_a^Y = \int_{-1}^1 G_H d\alpha' = G_{a1}^Y + G_{a2}^Y = \int_{-1}^1 (G_H - G_H^\Delta) d\alpha' + \int_{-1}^1 G_H^\Delta d\alpha', \quad (48)$$

$$G_b^Y = \int_{-1}^1 G_H \alpha' d\alpha' = G_{b1}^Y + G_{b2}^Y = \int_{-1}^1 (G_H - G_H^\Delta) \alpha' d\alpha' + \int_{-1}^1 G_H^\Delta \alpha' d\alpha', \quad (49)$$

$$G_c^Y = \int_{-1}^1 G_H \alpha'^2 d\alpha' = G_{c1}^Y + G_{c2}^Y = \int_{-1}^1 (G_H - G_H^\Delta) \alpha'^2 d\alpha' + \int_{-1}^1 G_H^\Delta \alpha'^2 d\alpha', \quad (50)$$

where

$$G_E^\Delta = \frac{1}{k_0 R}, \quad (51)$$

$$G_H^\Delta = \frac{1}{(k_0 R)^3} + \frac{1}{2k_0 R} - \frac{j}{3}. \quad (52)$$

The concept adopted in (44)-(50) is to split the corresponding integrands into two: one that is regular and can be numerically evaluated by a Gaussian quadrature (namely G_{a1}^{1Z} , G_{b1}^{1Z} , G_{a1}^{2Z} , G_{b1}^{2Z} , G_{a1}^Y , G_{b1}^Y , and G_{c1}^Y) and another that contains a removable singularity and can be integrated analytically (G_{a2}^{1Z} , G_{b2}^{1Z} , G_{a2}^{2Z} , G_{b2}^{2Z} , G_{a2}^Y , G_{b2}^Y and G_{c2}^Y). The latter integrals are given by [8]:

$$G_{a2}^{1Z} = \frac{2}{k_0 \Delta_q} I_G^1, \quad (53)$$

$$G_{b2}^{1Z} = \frac{4\alpha_0}{\Delta_q k_0} \left(\frac{2}{\alpha_4 + \alpha_5} - \frac{I_G^1}{\Delta_q} \right), \quad (54)$$

$$G_{a2}^{2Z} = \frac{I_G^2}{k_0 \beta_5}, \quad (55)$$

$$G_{b2}^{2Z} = 4 \frac{\beta_5 I_G^1 - \frac{\Delta_q}{2} \rho_q I_G^2}{\Delta_q^2 \sin u_q k_0 \beta_5}, \quad (56)$$

$$G_{a2}^Y = \frac{2}{k_0 \Delta_p} \alpha_1^H - j \frac{2}{3}, \quad (57)$$

$$G_{b2}^Y = \left(\frac{2}{k_0 \Delta_p} \right)^2 (\alpha_2^H - k_0 \alpha_0 \alpha_1^H), \quad (58)$$

$$G_{c2}^Y = \left(\frac{2}{k_0 \Delta_p} \right)^3 [\alpha_3^H - k_0 \alpha_0 (\alpha_2^H - k_0 \alpha_0 \alpha_1^H)] - j \frac{2}{9}, \quad (59)$$

where

$$\alpha_0 = (\rho_q - \rho) \sin u_q + (z_q - z) \cos u_q + 2\rho \sin u_q \sin^2 \left(\frac{\varphi}{2} \right), \quad (60)$$

$$\alpha_1 = |\alpha_0| + \frac{\Delta_q}{2} + \alpha_4, \quad (61)$$

$$\alpha_2 = |\alpha_0| - \frac{\Delta_p}{2} + \alpha_5, \quad (62)$$

$$\alpha_3 = \frac{\Delta_p}{2} - |\alpha_0| + \alpha_5, \quad (63)$$

$$\alpha_4 = \sqrt{\left(|\alpha_0| + \frac{\Delta_q}{2} \right)^2 + d_2^2}, \quad (64)$$

$$\alpha_5 = \sqrt{\left(|\alpha_0| - \frac{\Delta_q}{2} \right)^2 + d_2^2}, \quad (65)$$

$$\beta_1 = \frac{\Delta_q}{2} \left[\Delta_q \rho_q + 2\alpha_0 \left(\rho_q - \frac{\Delta_q}{2} \sin u_q \right) - 2d_m^2 \sin u_q \right], \quad (66)$$

$$\beta_2 = \frac{\Delta_q}{2} \left[\Delta_q \rho_q - 2\alpha_0 \left(\rho_q + \frac{\Delta_q}{2} \sin u_q \right) + 2d_m^2 \sin u_q \right], \quad (67)$$

$$\beta_3 = \rho_q + \frac{\Delta_q}{2} \sin u_q, \quad (68)$$

$$\beta_4 = \rho_q - \frac{\Delta_q}{2} \sin u_q, \quad (69)$$

$$\beta_5 = \frac{\Delta_q}{2} \sqrt{\rho_q^2 - 2\rho_q \sin u_q \alpha_0 + (\sin u_q d_m)^2}, \quad (70)$$

$$I_G^1 = \begin{cases} \ln \left(\frac{\alpha_1}{\alpha_2} \right), & |\alpha_0| \geq \frac{\Delta_q}{2} \\ \ln \left(\frac{\alpha_1 \alpha_2}{d^2} \right), & |\alpha_0| \leq \frac{\Delta_q}{2} \end{cases}, \quad (71)$$

$$I_G^2 = \ln \left[\left(\frac{\beta_2 + 2\alpha_5 \beta_5}{2\alpha_4 \beta_5 - \beta_1} \right) \frac{\beta_3}{\beta_4} \right], \quad (72)$$

$$\alpha_1^H = \frac{\Delta_q}{2(k_0 d)^2} \frac{1}{\alpha_4 \alpha_5} \left[\alpha_4 + \alpha_5 - \frac{4\alpha_0^2}{\alpha_4 + \alpha_5} \right] + \frac{1}{2} I_G^1, \quad (73)$$

$$\alpha_2^H = \frac{2k_0 \alpha_0 \Delta_q}{\alpha_4 + \alpha_5} \left[\frac{1}{2} + \frac{1}{k^2 \alpha_4 \alpha_5} \right], \quad (74)$$

$$\alpha_3^H = \frac{\Delta_q}{2} \left[(\alpha_4 + \alpha_5) \left(\frac{k^2}{4} - \frac{1}{\alpha_4 \alpha_5} \right) - \frac{(k_0 \alpha_0)^2}{\alpha_4 + \alpha_5} \right] + \left[1 - \frac{(k_0 d)^2}{4} \right] I_G^1, \quad (75)$$

$$R = \sqrt{\left(\frac{\alpha'_{\Delta_q}}{2} + \alpha_0 \right)^2 + d^2}, \quad (76)$$

$$d^2 = d_m - \alpha_0^2, \quad (77)$$

$$d_m = (\rho_q - \rho)^2 + (z_q - z)^2 + 4\rho_q \rho \sin^2 \left(\frac{\varphi}{2} \right). \quad (78)$$

After the singularity extraction by method 1, the remaining α and φ integrals are numerically evaluated by Gaussian quadratures.

B. Method 2

Method 2 is applied when the following condition is met:

$$R_c \leq C_\varphi \rho_q, \quad (79)$$

i.e., field and source segments are close to each other and both are distant from the symmetry axis. In this situation, due to large variation of R and to the relatively large value of ρ_q , the φ integrals must be numerically fortified in the limit $\varphi \rightarrow 0$ [4]. As the kernels of $G_4(t, t')$ and $G_6(t, t')$ are relatively well behaved, method 2 is only applied to the φ integrals in $G_1(t, t')$, $G_2(t, t')$, $G_3(t, t')$, and $G_5(t, t')$. In the limit $\varphi \rightarrow 0$, the kernels of (21)-(23) and (25) can be approximated by [8]:

$$\lim_{\varphi \rightarrow 0} \left[2 \sin^2 \left(\frac{\varphi}{2} \right) \cos m\varphi G_H \right] \approx \frac{\varphi^2}{2k_0^3} \left[(\rho - \rho')^2 + (z - z')^2 + \rho\rho'\varphi^2 \right]^{-3/2}, \quad (80)$$

$$\lim_{\varphi \rightarrow 0} [\cos \varphi \cos m\varphi G_H] \approx \frac{1}{k_0^3} [(\rho - \rho')^2 + (z - z')^2 + \rho\rho'\varphi^2]^{-3/2}, \quad (81)$$

$$\lim_{\varphi \rightarrow 0} [\sin \varphi \sin m\varphi G_H] \approx \frac{m\varphi^2}{k_0^3} [(\rho - \rho')^2 + (z - z')^2 + \rho\rho'\varphi^2]^{-3/2}, \quad (82)$$

$$\lim_{\varphi \rightarrow 0} [\cos \varphi \cos m\varphi G_E] \approx \frac{1}{k_0} [(\rho - \rho')^2 + (z - z')^2 + \rho\rho'\varphi^2]^{-1/2}. \quad (83)$$

Integration of (80)-(83) from $\varphi = 0$ to π provide:

$$I_1 = \frac{1}{2(k_0^2 \rho\rho')^{3/2}} \left[\frac{-v_1}{\sqrt{1+v_1^2}} + \ln(v_1 + \sqrt{1+v_1^2}) \right], \quad (84)$$

$$I_2 = \frac{\pi}{k_0^3} \frac{[(\rho - \rho')^2 + (z - z')^2]^{3/2}}{\sqrt{1+v_1^2}}, \quad (85)$$

$$I_3 = 2mI_1, \quad (86)$$

$$I_5 = \frac{1}{k_0 \sqrt{\rho\rho'}} \left[\ln(v_1 + \sqrt{1+v_1^2}) \right], \quad (87)$$

where

$$v_1 = \pi \sqrt{\frac{\rho\rho'}{(\rho - \rho')^2 + (z - z')^2}}. \quad (88)$$

The concept behind method 2 is to evaluate $G_1(t, t')$, $G_2(t, t')$, $G_3(t, t')$, and $G_5(t, t')$ using Gaussian quadrature but with the integrands of (21)-(23) and (25) subtracted by (80)-(83), respectively. Then, the analytical expressions of (84)-(87), respectively, are added. So, when method 2 is employed [8]:

$$G_1(t, t') = \frac{\pi}{2} \sum_{\beta=1}^{n_\phi} w_\beta \left\{ 2 \sin^2\left(\frac{\varphi_\beta}{2}\right) \cos m\varphi_\beta G_H - \frac{\varphi_\beta^2}{2k_0^3} [(\rho - \rho')^2 + (z - z')^2 + \rho\rho'\varphi_\beta^2]^{3/2} \right\} + I_1, \quad (89)$$

$$G_2(t, t') = \frac{\pi}{2} \sum_{\beta=1}^{n_\phi} w_\beta \left\{ \cos \varphi_\beta \cos m\varphi_\beta G_H - \frac{1}{k_0^3} [(\rho - \rho')^2 + (z - z')^2 + \rho\rho'\varphi_\beta^2]^{3/2} \right\} + I_2, \quad (90)$$

$$G_3(t, t') = \frac{\pi}{2} \sum_{\beta=1}^{n_\phi} w_\beta \left\{ \sin \varphi_\beta \sin m\varphi_\beta G_H - \frac{m\varphi_\beta^2}{k_0^3} [(\rho - \rho')^2 + (z - z')^2 + \rho\rho'\varphi_\beta^2]^{-3/2} \right\} + I_3, \quad (91)$$

$$G_5(t, t') = \frac{\pi}{2} \sum_{\beta=1}^{n_\phi} w_\beta \left\{ \cos \varphi_\beta \cos m\varphi_\beta G_E - \frac{1}{k_0} [(\rho - \rho')^2 + (z - z')^2 + \rho\rho'\varphi_\beta^2]^{-1/2} \right\} + I_5, \quad (92)$$

where

$$\varphi_\beta = (\alpha_\beta + 1)\frac{\pi}{2}, \tag{93}$$

α_β and w_β are the abscissas and the weights of the Gaussian quadrature with n_φ points, respectively.

After the singularity extraction by method 2, the remaining α and α' integrals of $G_1(t, t')$, $G_2(t, t')$, $G_3(t, t')$, and $G_5(t, t')$ are numerically evaluated by Gaussian quadratures.

C. Method 3

Method 3 is used instead of methods 1 and 2 whenever the source segment coincides with the observation segment. In this case the kernels of $G_4(t, t')$ and $G_6(t, t')$ are well behaved and the expression containing $G_2(t, t')$ ends up being multiplied by zero. Thus the method is only applied to the integration of (21), (23), and (25) (i.e., $G_1(t, t')$, $G_3(t, t')$, and $G_5(t, t')$) with respect to α' and φ . In this situation, the singularities occur when $\alpha \rightarrow \alpha'$ and $\varphi \rightarrow 0$. In these limits, the integrands of $G_1(t, t')$, $G_3(t, t')$, and $G_5(t, t')$ can be approximated by [8]:

$$G_{1M3} = \lim_{\substack{\varphi \rightarrow 0 \\ \alpha \rightarrow \alpha'}} \left[2 \sin^2\left(\frac{\varphi}{2}\right) \cos m\varphi G_H \right] \approx \frac{\varphi^2}{2k_0^3} \left[\frac{\Delta_q^2}{4} (\alpha - \alpha')^2 + \rho_q^2 \varphi^2 \right]^{-3/2}, \tag{94}$$

$$G_{3M3} = \lim_{\substack{\varphi \rightarrow 0 \\ \alpha \rightarrow \alpha'}} \left[\sin \varphi \sin m\varphi G_H \right] \approx \frac{m\varphi^2}{k_0^3} \left[\frac{\Delta_q^2}{4} (\alpha - \alpha')^2 + \rho_q^2 \varphi^2 \right]^{-3/2} \approx 2mG_{1M3}, \tag{95}$$

$$G_{5M3} = \lim_{\substack{\varphi \rightarrow 0 \\ \alpha \rightarrow \alpha'}} \left[\cos \varphi \cos m\varphi G_E \right] \approx \frac{1}{k_0} \left[\frac{\Delta_q^2}{4} (\alpha - \alpha')^2 + \rho_q^2 \varphi^2 \right]^{-1/2}. \tag{96}$$

Method 3 evaluates $G_1(t, t')$, $G_3(t, t')$, and $G_5(t, t')$ in (21), (23), and (25), respectively, using the previous method 1. The results are then subtracted by the integrals of (94)-(96) with respect to α' (analytical solution) and φ (numerical solution) respectively. Finally, the analytical integrals of (94)-(96) with to φ and α' are respectively added [8]. The necessary analytical integrations of (94)-(96) to be used in (13)-(20) are [8]:

$$\int \int_{\varphi \alpha'} G_{1M3} d\alpha' d\varphi = \frac{1}{4k_0^3 \rho_q^3} \left\{ -\ln \left[(\alpha - 1)^2 \Delta_q^2 \right] - \ln \left[(\alpha + 1)^2 \Delta_q^2 \right] + \alpha \ln \left[\frac{(\alpha - 1)^2}{(\alpha + 1)^2} \right] \right. \\ \left. + 2 \ln \left[2\pi\rho_q \left(1 + \sqrt{1 + p_1^2} \right) \right] + 2 \ln \left[2\pi\rho_q \left(1 + \sqrt{1 + p_2^2} \right) \right] + 2\alpha \ln \left[\frac{1 + \sqrt{1 + p_2^2}}{1 + \sqrt{1 + p_1^2}} \right] \right\}, \tag{97}$$

$$\int\int_{\varphi \alpha'} G_{1M3} \alpha' d\alpha' d\varphi = \frac{1}{8k_0^3 \Delta_q^2 \rho_q^3} \left\{ 8\pi^2 \rho_q^2 \left[\sqrt{1+p_2^2} - \sqrt{1+p_1^2} \right] + (\alpha^2 - 1) \Delta_q^2 \left[\ln \left[\frac{(\alpha-1)^2}{(\alpha+1)^2} \right] + 2 \ln \left[\frac{1+\sqrt{1+p_2^2}}{1+\sqrt{1+p_1^2}} \right] \right] \right\}, \tag{98}$$

$$\int\int_{\varphi \alpha'} G_{1M3} \alpha'^2 d\alpha' d\varphi = \frac{\pi^2}{6k_0^3 \Delta_q^3 \rho_q^3} \left\{ 4\Delta_q \left[\sqrt{1+p_2^2} (2\alpha-1) - \sqrt{1+p_1^2} (2\alpha+1) \right] + 8\pi\rho_q \ln \left[\frac{-p_1 + \sqrt{1+p_1^2}}{-p_2 + \sqrt{1+p_2^2}} \right] \right\} + \frac{1}{12k_0^3 \rho_q^3} \left\{ -\ln \left[(\alpha-1)^2 \Delta_q^2 \right] - \ln \left[(\alpha+1)^2 \Delta_q^2 \right] + \alpha^3 \ln \left[\frac{(\alpha-1)^2}{(\alpha+1)^2} \right] + 2 \ln \left[2\pi\rho_q \left(1 + \sqrt{1+p_1^2} \right) \right] + 2 \ln \left[2\pi\rho_q \left(1 + \sqrt{1+p_2^2} \right) \right] + \alpha^3 \ln \left[\frac{1+\sqrt{1+p_2^2}}{1+\sqrt{1+p_1^2}} \right] \right\}, \tag{99}$$

$$\int\int_{\varphi \alpha'} G_{3M3} d\alpha' d\varphi = 2m \int\int_{\varphi \alpha'} G_{1M3} d\alpha' d\varphi, \tag{100}$$

$$\int\int_{\varphi \alpha'} G_{3M3} \alpha' d\alpha' d\varphi = 2m \int\int_{\varphi \alpha'} G_{1M3} \alpha' d\alpha' d\varphi, \tag{101}$$

$$\int\int_{\varphi \alpha'} G_{3M3} \alpha'^2 d\alpha' d\varphi = 2m \int\int_{\varphi \alpha'} G_{1M3} \alpha'^2 d\alpha' d\varphi, \tag{102}$$

$$\int\int_{\varphi \alpha'} G_{5M3} d\alpha' d\varphi = \frac{1}{k_0 \Delta_q \rho_q} \left\{ \Delta_q \ln(64) + \Delta_q \left[(\alpha-1) \ln(4\Delta_q |\alpha-1|) - (\alpha+1) \ln(4\Delta_q |\alpha+1|) - (\alpha-1) \ln \left[\left| \frac{(\alpha-1)\Delta_q}{2} \right| \left(\frac{1}{p_1} + \sqrt{1+\frac{1}{p_1^2}} \right) \right] + (\alpha+1) \ln \left[\left| \frac{(\alpha+1)\Delta_q}{2} \right| \left(\frac{1}{p_2} + \sqrt{1+\frac{1}{p_2^2}} \right) \right] \right] + 2\pi\rho_q \left[-\ln \left(\frac{|\alpha-1|}{|\alpha-1| + \sqrt{1+\frac{1}{p_1^2}}} \right) + \ln \left(\frac{|\alpha+1|}{|\alpha+1| + \sqrt{1+\frac{1}{p_2^2}}} \right) + \ln \left[\frac{|\alpha+1|}{|\alpha-1|} \right] \right] \right\}, \tag{103}$$

$$\begin{aligned}
 \iint_{\varphi \alpha'} G_{5M3} \alpha' d\alpha' d\varphi = & \frac{1}{2k_0 \Delta_q \rho_q} \left\{ 2\pi \rho_q \left[|\alpha-1| \sqrt{1+\frac{1}{p_1^2}} - |\alpha+1| \sqrt{1+\frac{1}{p_2^2}} \right] \right. \\
 & + \Delta_q^2 \left[(\alpha^2-1) \ln(4\Delta_q |\alpha-1|) + (1-\alpha^2) \ln(4\Delta_q |\alpha+1|) \right. \\
 & + (1-\alpha^2) \Delta_q \left[\ln\left(\frac{1}{p_1} + \sqrt{1+\frac{1}{p_1^2}}\right) + \ln\left(\frac{|\alpha-1| \Delta_q}{2}\right) \right] \\
 & \left. \left. + (\alpha^2-1) \Delta_q \left[\ln\left(\frac{1}{p_2} + \sqrt{1+\frac{1}{p_2^2}}\right) + \ln\left(\frac{|\alpha+1| \Delta_q}{2}\right) \right] \right] \right\} \\
 & + 4\pi \alpha \rho_q \left[\ln\left(\frac{\alpha+1}{|\alpha+1|} + \sqrt{1+\frac{1}{p_2^2}}\right) - \ln\left(\frac{\alpha-1}{|\alpha-1|} + \sqrt{1+\frac{1}{p_1^2}}\right) + \ln\left(\frac{|\alpha+1|}{|\alpha-1|}\right) \right] \Bigg\}, \quad (104)
 \end{aligned}$$

where

$$p_1 = \frac{(\alpha-1) \Delta_q}{2\rho_q \pi}, \quad (105)$$

$$p_2 = \frac{(\alpha+1) \Delta_q}{2\rho_q \pi}, \quad (106)$$

IV. NUMERICAL RESULTS

To demonstrate the usefulness of the singularity-extraction techniques presented in the previous section, the electromagnetic scattering of a plane wave by spherical PEC, dielectric, and composed bodies are investigated. The BOR geometries are those illustrated in the Fig. 2. Their (external) radii of the spheres were varied from $0.5\lambda_0$ to $50\lambda_0$. The dielectric relative permittivity (ϵ_r) was varied up to 50. Whenever possible, the precision of the numerical results was verified against analytical solutions based on Mie series [14] using the following relative mean error:

$$E_{MR} (\%) = \frac{E_{Rr} + E_{Rj\phi} + E_{RM_r} + E_{RM_\phi}}{4}, \quad (107)$$

where E_{RX} represents the relative mean error of the current X component as

$$E_{RX} (\%) = 100 \frac{|\mathbf{X}^{MoM} - \mathbf{X}^{Mie}|_{\max}}{|\mathbf{X}^{Mie}|_{\max}}, \quad (108)$$

with X representing any one of the electric (J_r or J_ϕ) or magnetic (M_r or M_ϕ) current components and \mathbf{X}^{MoM} and \mathbf{X}^{Mie} representing the numerical and analytical solutions, respectively.

To illustrate the usefulness of the singularity extraction discussed in Sect. III, all case studies discussed below present two different numerical results: one with the application of the singularity

extraction technique and another without it. In the latter, divisions by zero are artificially avoided by using different numbers of points for the Gaussian quadratures corresponding to the α and α' integrals (3 and 2 points for the Gaussian quadratures corresponding to the α and α' integrals, respectively). When the singularity extraction is applied, a 2-point Gaussian quadrature is used for both integrals.

The first case study deals with the plane-wave scattering by a PEC sphere with radius $a = 50\lambda_0$, as illustrated in Fig. 2(a). The normalized J_t and J_ϕ amplitudes of the surface electric current are illustrated in Fig. 3 as functions of the length $S(\lambda_0)$ measured along the sphere generatrix (such that $S = 0$ corresponds to the farthest left point). In this particular case study the numerical results were obtained by the CFIE formulation (as we have here a closed PEC object) with 1,177 TBF's to represent each J_t and J_ϕ current components (i.e., 1,178 segments were used to represent the sphere generatrix). Without the singularity extraction the currents were calculated with $E_{MR} = 1.34\%$ (dashed lines in Fig. 3). With the singularity extraction, $E_{MR} = 0.93\%$ and the time spent to fill the MoM Z-matrix is decreased by about 30% (because both α and α' quadratures use only 2 points).

In the second example the PEC sphere is substituted by a dielectric one with $a = 10\lambda_0$ and $\epsilon_r = 50$, as illustrated in Fig. 2(a). The normalized current amplitudes of the electric J_t and magnetic M_t components are illustrated in Fig. 4 (J_ϕ and M_ϕ are not shown). The numerical results were obtained by the Müller formulation [7]-[11] using 941 TBF's to represent each one of the four current components (i.e., 942 segments were used to represent the generatrix of the sphere). Without the singularity extraction (dashed lines in Fig. 4) $E_{MR} = 17.09\%$. However, when the technique is applied the relative error is considerably improved ($E_{MR} = 1.13\%$).

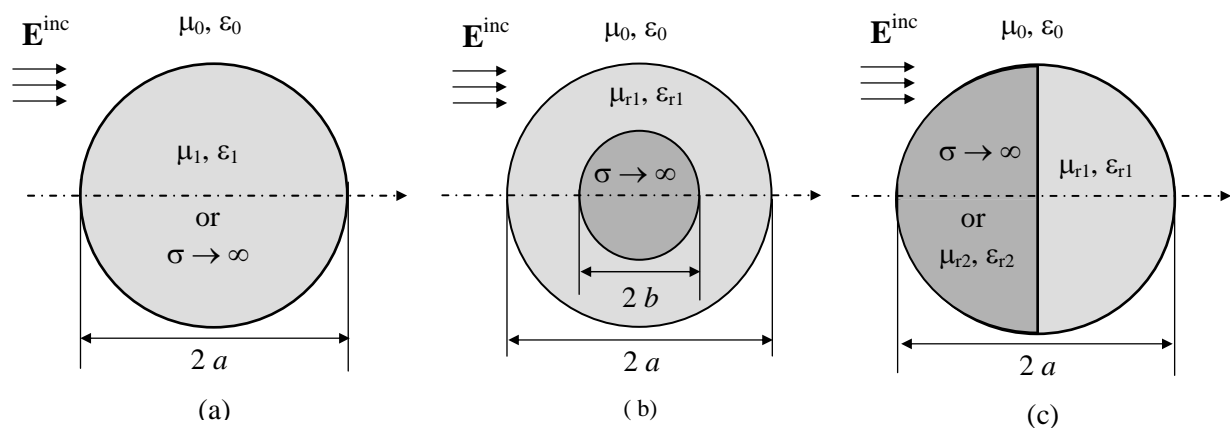


Fig. 2. Geometries analyzed in this work: (a) homogeneous sphere, (b) PEC sphere covered by a dielectric layer and (c) sphere composed by two homogeneous hemispheres.

The third case study investigates the plane-wave scattering by a PEC sphere (with radius $b = 10\lambda_0$) covered by a dielectric layer with external radius $a = 11\lambda_0$ and $\epsilon_r = 20$, as illustrated in Fig. 2(b). The numerical results were obtained by the CFIE (over the PEC spherical surface) and by the Müller formulation (over the dielectric surface) [7],[8]. Each current component was represented by 1,099 TBF's on each PEC and dielectric surfaces. Figure 5 illustrates the normalized equivalent current amplitudes of the electric J_t and magnetic M_t components over the dielectric sphere (the J_t and J_ϕ currents over the PEC sphere and the J_ϕ and M_ϕ currents over the dielectric sphere are not shown). When the singularity extraction is not used, $E_{MR} = 40.09\%$. But the relative error improves to $E_{MR} = 1.24\%$ when the singularity extraction is employed.

The last example deals with the plane-wave scattering by a composite sphere, like the one illustrated in Fig. 2(c). However, in the present study both hemispheres are made of the same dielectric material (with $a = 20\lambda_0$ and $\epsilon_{r1} = \epsilon_{r2} = 4$). So, it is actually a homogeneous dielectric sphere, for which an analytical solution based on Mie series is attained and used to estimate the E_{MR} of the MoM solutions. The motivation here is to investigate possible problems related to the numerical treatment of the equivalent currents around junctions among different media. The numerical results were obtained by PMCWHT formulation [7]-[13] using 942 TBF's to represent each one of the four equivalent current components over the external spherical surface. Figure 6 illustrates the normalized equivalent current amplitudes of the electric J_t and magnetic M_t components over the external surface. When the singularity extraction is not adopted, $E_{MR} = 6.39\%$. But E_{MR} improves to 0.49% when the singularity extraction is used.

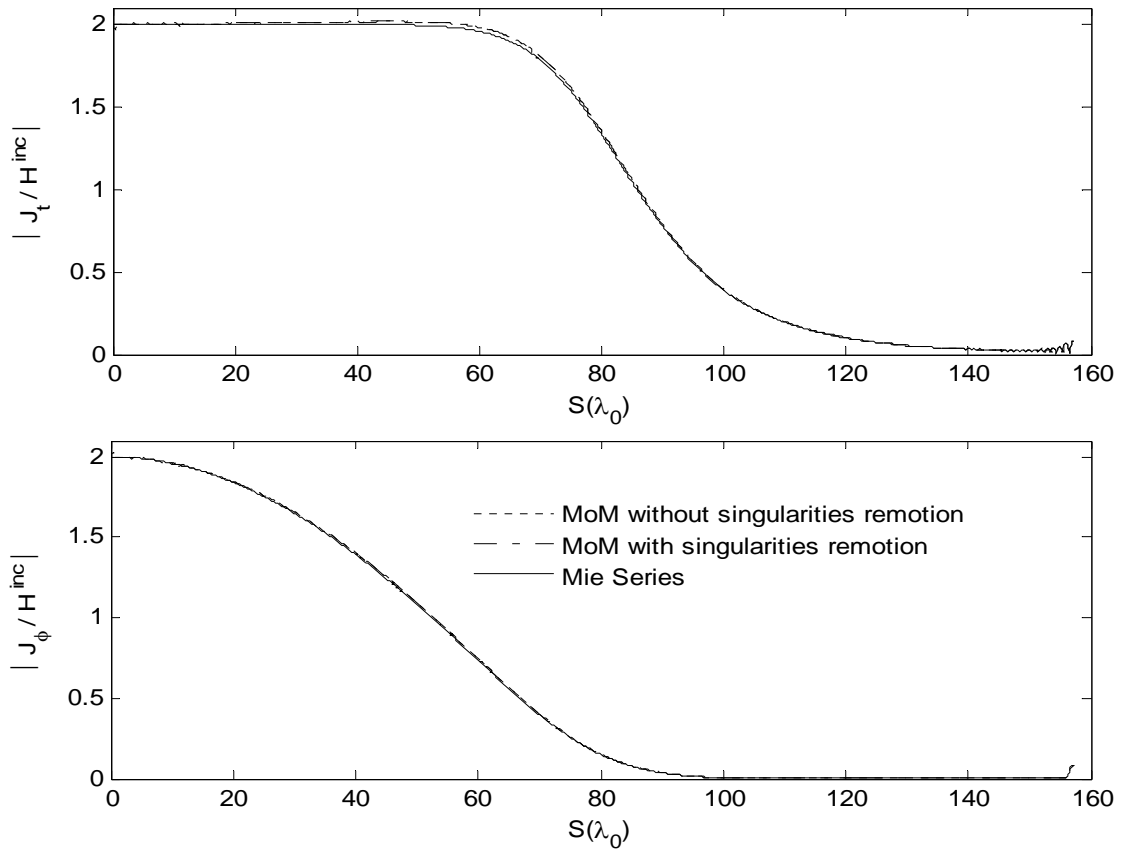


Fig. 3. Surface electric current over the PEC sphere with radius $a = 50\lambda_0$.

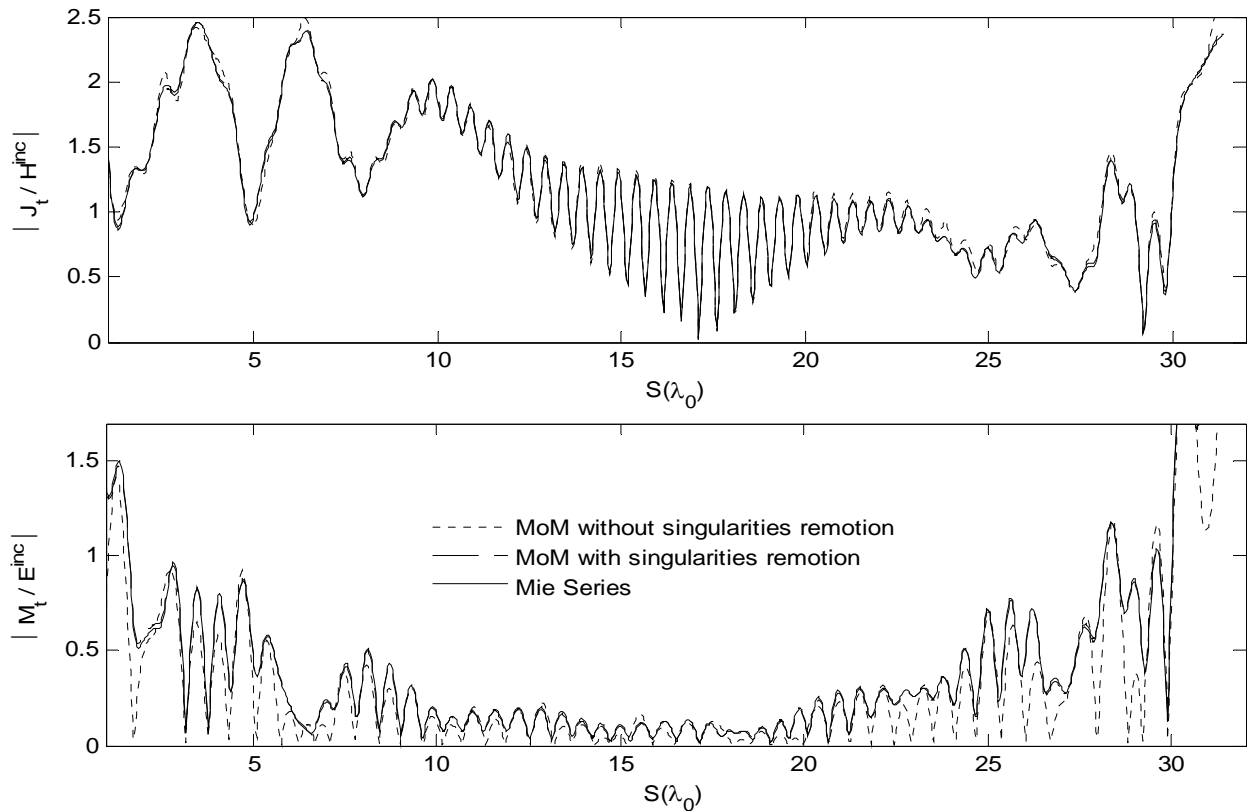


Fig. 4. Equivalent surface electric current over the dielectric sphere with radius $a = 10\lambda_0$ and $\epsilon_r = 50$.

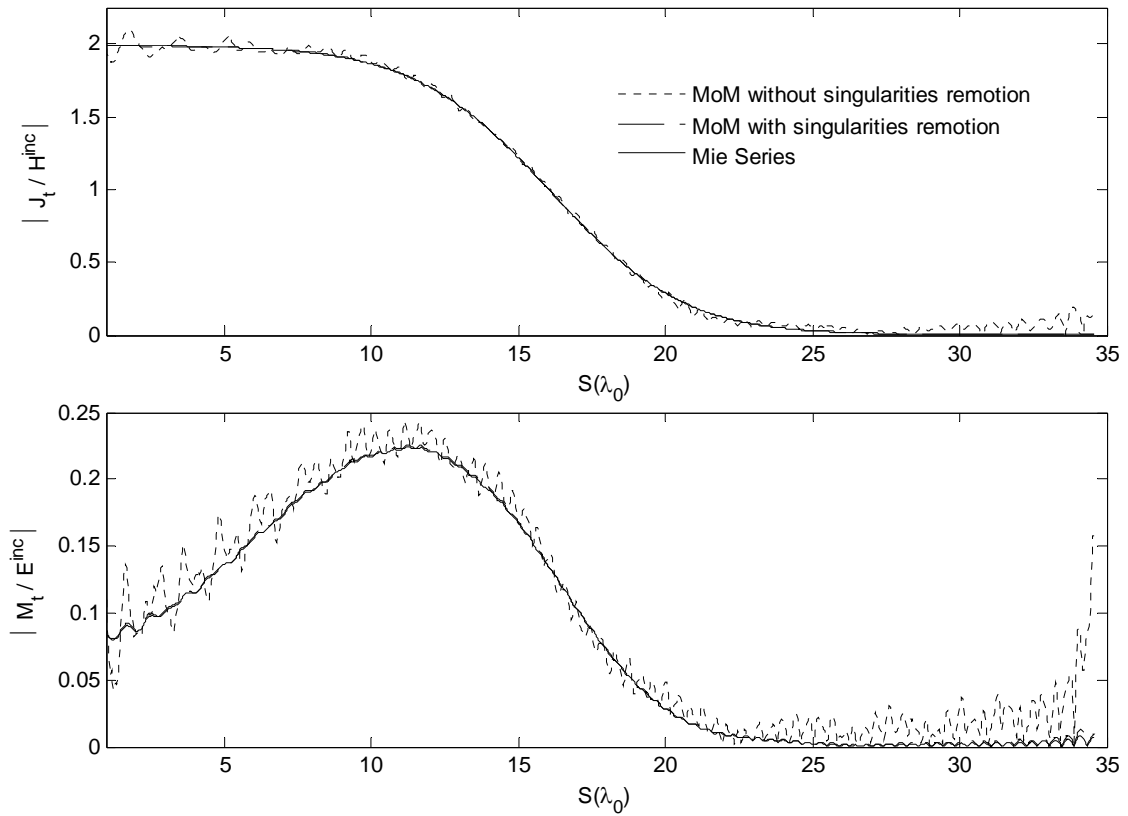


Fig. 5. Equivalent electric and magnetic surface currents over the dielectric surface of a PEC sphere with radius $b = 10\lambda_0$ covered by a dielectric layer with radius $a = 11\lambda_0$ and $\epsilon_r = 20$.

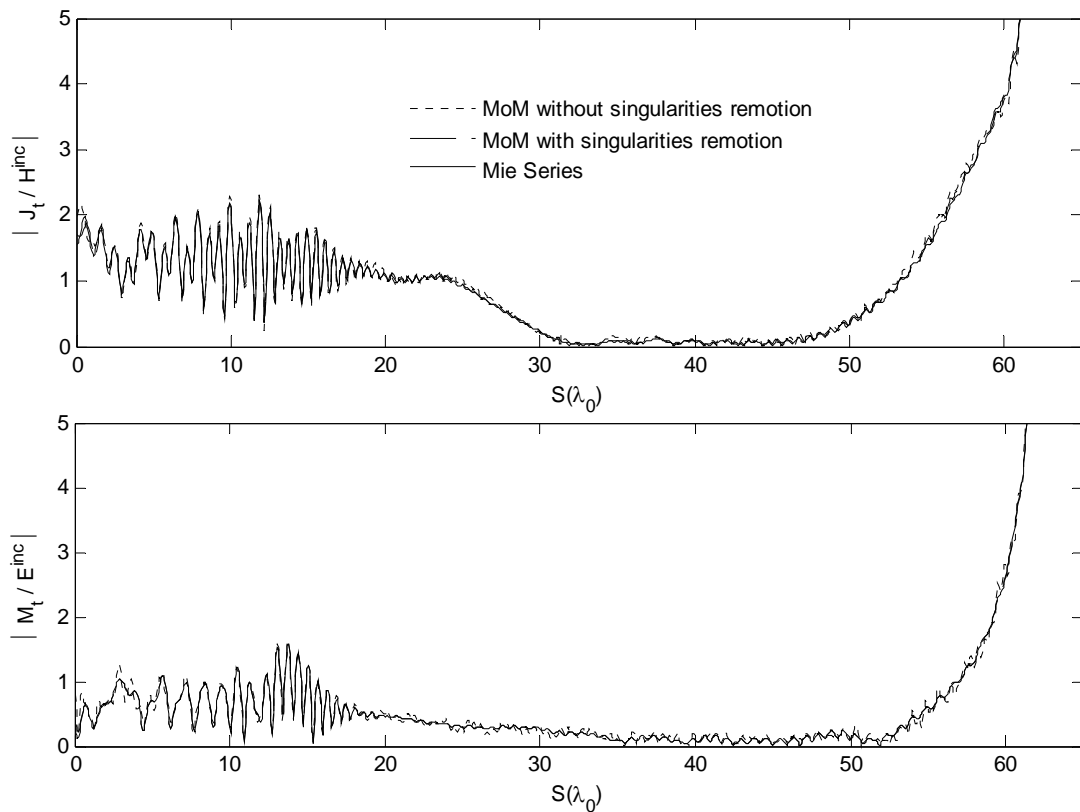


Fig. 6. Equivalent electric and magnetic surface currents over the external surface of the composite sphere of Fig. 2(c) with radius $a = 20\lambda_0$ and $\epsilon_{r1} = \epsilon_{r2} = 4$.

V. CONCLUSIONS

This work evaluated electromagnetic scattering by PEC, dielectric, and composite spheres using MoM. It was presented an accurate and robust numerical process to deal with the singularities arising in the integrals in the elements of Z and Y matrices. By this technique the singularities were extracted and evaluated analytically. Numerical integration by Gaussian quadrature was only applied to the regular part of the kernels. The choice of basis functions to represent current behavior was very important for the accuracy and convergence of the numerical analysis. In this work this representation was carried by triangular TBF functions, which ensures a good representation of the current behavior and produce relatively simple integral equations. In all carried tests accurate numerical results had been obtained when the singularities removal technique was used. It was demonstrated that the appropriate treatment of the integrals singularities is capable of reducing the number of basis functions required to represent the surface current behavior.

REFERENCES

- [1] M. S. Ingber and R. H. Ott, "An application of the boundary element method to the magnetic field integral equation," *IEEE Trans. Antennas and Propagation*, vol. 39, pp. 606-611, May 1991.
- [2] J. R. Mautz, "A stable integral equation for electromagnetic scattering from homogeneous dielectric bodies," *IEEE Trans. Antennas and Propagation*, vol. 37, pp. 1070-1071, August 1987.
- [3] A. W. Glisson, "On the development of numerical techniques for treating arbitrarily-shaped surfaces," Ph.D. Dissertation, University of Mississippi, June 1975.
- [4] J. R. Mautz and R. F. Harrington, "An improved E-Field solution for a conducting body of revolution," Tech. Report TR-80-1, Dept. Electrical and Computer Engineering, Syracuse University, 1980.
- [5] F. J. S. Moreira, "Design and Rigorous Analysis of Generalized Axially Symmetric Dual-Reflector Antennas", Ph.D. Dissertation, University of Southern California, August 1997.
- [6] J. R. Mautz and R. F. Harrington, "H-Field, E-Field and combined field solutions for bodies of revolution," Tech. Report TR-77-2, Dept. Electrical Computer Engineering, Syracuse University, 1977.
- [7] J. R. Mautz and R. F. Harrington, "Electromagnetic scattering from a homogeneous body of revolution," Tech. Report TR-77-10, Dept. Electrical and Computer Engineering, Syracuse University, 1977.
- [8] U. C. Resende, *Análise de antenas refletoras circularmente simétricas com a presença de corpos dielétricos*, Doctorate Thesis, Dept. of Electronics Engineering, UFMG, Minas Gerais, Brazil, May 2007.
- [9] U. C. Resende, F. J. S. Moreira, O. M. C. P. Filho and J. A. Vasconcelos, "Optimal Number of Basis Functions in the MoM Solutions for Bodies of Revolution," *Journal of Microwaves and Optoelectronics*, vol. 6, no. 1, pp. 220-235, June 2007.
- [10] P. Ylä-Oijala and M. Taskinen, "Calculation of CFIE impedance matrix elements with RWG and $n \times$ RWG functions," *IEEE Trans. Antennas and Propagation*, vol. 51, no. 8, pp. 1837-1846, August 2003.
- [11] P. Ylä-Oijala and M. Taskinen, "Well-conditioned Müller formulation for electromagnetic scattering by dielectric objects," *IEEE Trans. Antennas and Propagation*, vol. 53, no. 10, pp. 3316-3323, Oct. 2005.
- [12] L. N. M. Mitschang and J. M. Putman, "Electromagnetic scattering from axially inhomogeneous bodies of revolution," *IEEE Trans. Antennas and Propagation*, vol. 32, no. 8, pp. 797-806, August 1984.
- [13] S. Chen, J. S. Zhao, W. C. Chew, "Analyzing low-frequency electromagnetic scattering from a composite object," *IEEE Trans. Antennas and Propagation*, vol. 40, no. 2, pp. 426-433, February 2002.
- [14] G. Mie, "Beitrag zur optik trüber medien, speziell kolloider metallo-sungen," *Ann. Phys.*, vol 25, p. 377, 1908.